Group delay and dispersion in adiabatic plasmonic nanofocusing

Vasily Kravtsov, Joanna M. Atkin, and Markus B. Raschke*

Department of Physics, Department of Chemistry, and JILA, University of Colorado, Boulder, Colorado 80309, USA
**Corresponding author: markus.raschke@colorado.edu*

Received February 4, 2013; revised March 5, 2013; accepted March 7, 2013;
posted March 21, 2013 (Doc. ID 184800); published April 12, 2013

We study the decrease in group velocity of broadband surface plasmon polariton propagation on a conical tip, using femtosecond time-domain interferometry. The group delay of (9 ± 3) fs measured corresponds to a group velocity at the apex of less than $0.2c$. The result agrees in general with the prediction from adiabatic plasmonic nanofocusing theory, yet is sensitive with respect to the exact taper geometry near the apex. This, together with the sub 25 fs^2 second-order dispersion observed, provides the fundamental basis for the use of plasmons for broadband slow-light applications. © 2013 Optical Society of America

OCIS codes: 240.6680, 120.3180.

The manipulation of the speed of light has important applications for the control of laser pulse propagation, optical switching, and time synchronization. Soliton formation, superluminal propagation, and slow light [1,2] in metamaterials and highly nonlinear media is of fundamental and technological interest. Furthermore, slow light can enhance the light-matter interaction and amplify nonlinear responses [3].

Typically, the speed of light is controlled via the resonant dispersion in a material, where large changes in the refractive index occur within a narrow spectral range. An alternative approach takes advantage of the nonresonant group velocity dispersion in waveguides or metamaterial dielectric stacks [4]. Both approaches rely on maximizing the group velocity change while minimizing pulse distortion arising from higher-order dispersion, therefore limiting slow light to narrow bandwidths and long pulse durations.

Surface plasmon polaritons (SPPs), conversely, can intrinsically be broadband [5,6]. Slow SPPs with group velocities close to zero for narrow wavelength ranges have been demonstrated in specially tailored periodic structures [7]. Slow light can also be achieved via the transformation and confinement of SPP modes in certain tapered geometries, where they experience an increasing index of refraction over a broad spectral range [8,9].

One such geometry for ultrashort three-dimensional slow-light propagation is a conical taper, where the predicted decrease in group velocity v_g allows for optical nanofocusing far beyond the far-field diffraction limit [10,11]. However, the evidence for the decrease in v_g has only been indirect through the spatial nanofocusing properties, making the comparison with theory regarding the proposed microscopic mechanism difficult [12,13].

In this Letter, we directly measure the increase in propagation time of SPPs as they approach the apex of a conical tip by femtosecond time-domain interferometry, confirming the predicted decrease of v_g during adiabatic nanofocusing. This result is important for the optimization of nanofocusing applications, including broadband absorbers [14] and light harvesting devices [9].

Previous work has measured group velocity and dispersion associated with SPP propagation on noble metal nanowires [15,16], dielectric photonic waveguides [17], and plasmonic waveguides [18,19]. A reduced v_g has been observed for Au nanowires with radii <100 nm [15]. While a conical tip can be viewed as a semi-infinite nanowire with a continuously decreasing radius, it is not *a priori* clear if the group delay results for nanowires directly apply to the conical geometry.

For our experiments, we use an interferometric technique conceptually similar to that in [15] to study the continuous change of group velocity experienced by SPP modes propagating on a tip. We fabricate conical tips from 125 μm diameter gold wire (Advent) by electrochemical etching described in [20], with half-apical angle 7°–10° and apex radius ~10–20 nm. Grooves with dimensions optimized for coupling 790 nm laser light into SPPs are engraved on the tip surface by focused ion beam milling [21] at 20 and 40 μm distance from the apex as shown in Fig. 1(a). The tips are mounted on a piezostage allowing us to illuminate the top groove (G_1) or the

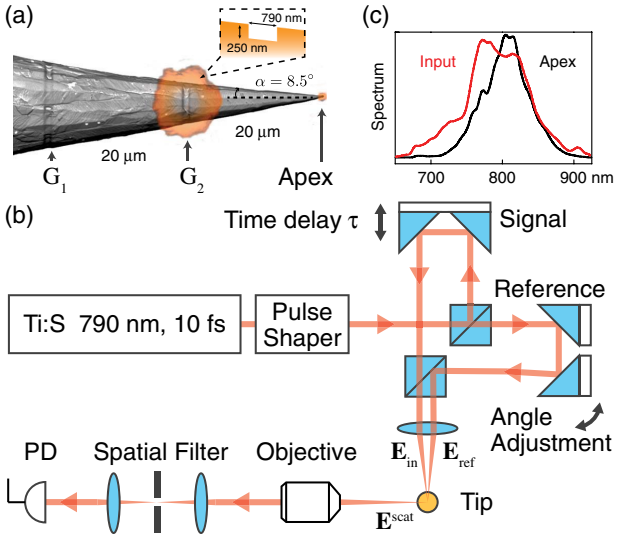

Fig. 1. (Color online) (a) Superimposed optical and SEM images of a Au tip with two grooves for launching SPPs, inset shows groove dimensions. (b) Setup to measure the decrease of the SPP group velocity with noncollinear pulse pair generation and femtosecond interferometry using a Mach–Zehnder type interferometer. (c, red) Laser excitation spectrum and (c, black) nanofocused apex emission spectrum.

bottom groove (G_2) without the need to realign the illumination or detection optics.

SPPs are launched using a Ti:sapphire oscillator (FemtoLasers, ~10 fs pulse duration). A Mach–Zehnder type interferometer generates pulse pairs $\mathbf{E}_{in}$ and $\mathbf{E}_{ref}$ with controlled time delay τ as shown in Fig. 1(b). The two pulses propagate noncollinearly and are focused by a $f = 20$ mm achromatic lens at two separate locations on the tip surface. To achieve the shortest possible pulse duration in the laser foci, we compensate for dispersion with a pulse shaper, implementing a multiphoton intrapulse interference phase scan (MIIPS) algorithm [22]. Tip-scattered light is collected using a microscope objective (50X/NA = 0.50, Olympus) in a 90° sagittal geometry, spatially filtered, and detected with a photodiode as a function of τ. An incident laser spectrum (red line) and apex SPP emission spectrum (black) are shown in Fig. 1(c), demonstrating the broadband nature of the nanofocusing process.

As shown schematically in Fig. 2 (top, right), we first focus the signal beam $\mathbf{E}_{in}$ onto G_1 to launch a propagating SPP, which scatters into far-field radiation $\mathbf{E}_{SPP}^{scat}$ at G_2. $\mathbf{E}_{SPP}^{scat}$ interferes with the scattered field $\mathbf{E}_{ref}^{scat}$ of the reference beam focused onto G_2. This gives rise to an interferogram $I^{scat}(\tau) = |\mathbf{E}_{SPP}^{scat} + \mathbf{E}_{ref}^{scat}|^2$ as a function of time delay τ ($G_1 \rightarrow G_2$, red). This defines the reference SPP group velocity, where the radius is large and the SPPs do not experience any nanofocusing. We then raise the tip by 20 μm to excite a propagating SPP at G_2 (bottom), and detect the interference between the nanofocused SPP emission from the apex and the apex-scattered reference light ($G_2 \rightarrow$ apex, blue).

To determine the time delay between the two interferograms, we calculate their Fourier transforms, select a sideband in frequency space, and derive the envelope function (dashed lines) from the inverse Fourier transform. The time interval between the maxima of the two envelopes $\tau_c = t_2 - t_1$ reflects the group delay due to the decrease of the group velocity during nanofocusing. From repeated experiments with the same tip, we obtain an average value with statistical error of $\tau_c = (9 \pm 3)$ fs,

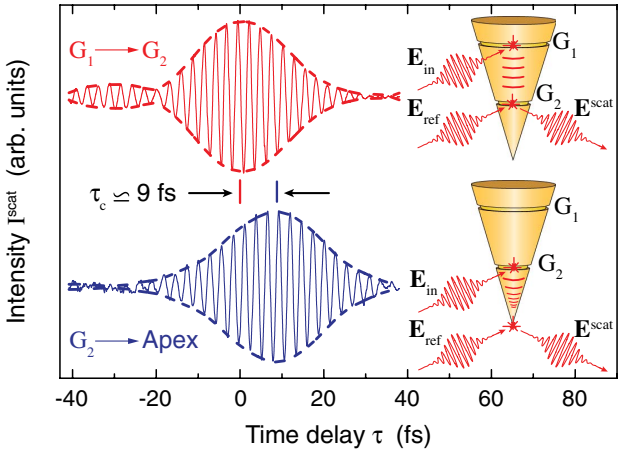

Fig. 2. (Color online) Interferograms for the SPP launched at G_1 with reference arm focus at G_2 (top, red). SPP launched at G_2, nanofocusing at the apex, with reference at the apex (bottom, blue), experiencing a group delay of $\tau_c \simeq 9$ fs.

Table 1. Measured SPP Group Delay for Adiabatic Nanofocusing on Different Au Tips with Combined Statistical and Systematic Uncertainties

	Group Delay $\tau_c \pm \delta\tau$	
Tip 1	9 ± 3 fs	Single groove
Tip 2	-4 ± 3 fs	Single groove
Tip 3	15 ± 8 fs	Double groove

as shown in Table 1 together with the results for two other tips for reference. The variation indicates that the delay is highly sensitive to details of tip geometry. For example, measurements on tip 2 produce an essentially zero delay within uncertainty. For tip 3 we fabricated double grooves to achieve higher SPP coupling efficiency (also dependent on groove dimensions), resulting in a better signal but a larger systematic uncertainty with respect to spatial location for SPP excitation and emission.

For comparison, we calculate the expected time delay based on the adiabatic model of plasmon nanofocusing on a gold cone [11]. We numerically obtain the spatial dispersion of effective index of refraction n_e and group velocity $v_g/c = [d(n_e\omega)/d\omega]^{-1}$ upon SPP propagation toward the apex. While the cone can support several cylindrical plasmonic modes ($m = 0, 1, 2\ldots$), only the lowest order symmetric mode ($m = 0$) experiences nanofocusing. In addition to $m = 0$, higher-order modes will propagate between G_1 and G_2, up to $m = 3$ for the tip geometries used in the experiment. While these modes have a slightly lower v_g than the $m = 0$ mode, their differences in group velocity translate into group delays not exceeding 0.2 fs, allowing us to limit our consideration to the $m = 0$ mode. As shown in Fig. 3(a), the $m = 0$ SPP group velocity decrease with propagation toward the geometric apex is more pronounced for smaller cone half-angles α. The group delay calculated for the $m = 0$ mode is shown in Fig. 3(b) as a function of apex radius, which defines the point where the SPP re-emits into the far field.

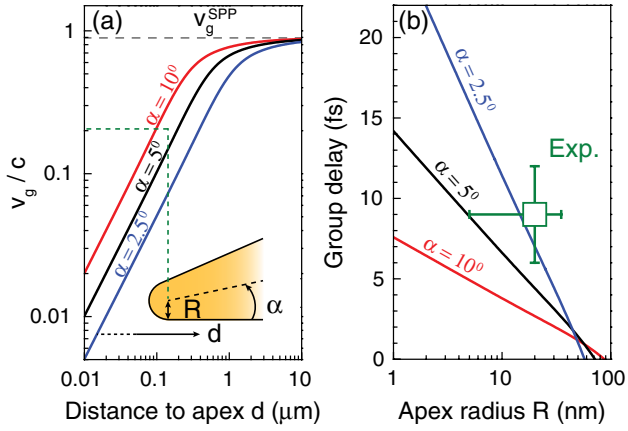

Fig. 3. (Color online) (a) Calculated group velocity v_g decrease for SPP propagation on Au tips for different cone angles, with $v_g^{SPP} \simeq 0.9c$ for a planar SPP at 1.5 eV (grey dashed). Decrease to $v_g \sim 0.2c$ expected at the apex for the tips in our experiment (green dashed, $\alpha \sim 8.5°$). (b) Corresponding apex radius dependence of SPP group delay for the experimental configuration, with measured value (green symbol).

Our measured value of the group delay of $\tau_c = (9 \pm 3)$ fs (green symbol), taking into account our knowledge of the tip radius from SEM, is somewhat larger than that expected theoretically (solid lines). This deviation is unsurprising considering that v_g starts to change appreciably only within a few 100 nm proximity from the apex [Fig. 3(a)]. Here, concomitant with the actual tip geometry deviating increasingly from the ideal conical shape toward the apex, the change in v_g becomes very sensitive to the exact geometry. In addition, the theory does not account for finite size effects in the dielectric function for small tip radii, surface roughness, and reduced losses due to nonlocality in the dielectric response [23,24].

The measured group delay is the cumulative effect of the continuous decrease in group velocity. Based on the model we expect $v_g \sim 0.2c$ at the apex [Fig. 3(a), green dashed line]. However, given the larger than predicted experimental group delay (b), the SPP at the apex may be even slower.

Nanofocusing is a low dispersion process, so that the SPP pulse experiences minimal temporal distortion. Based on measurement of the exact optical transient in the nanofocus by frequency-resolved optical gating [25], we estimate that the second-order dispersion introduced through propagation and nanofocusing is less than 25 fs^2. This is consistent with values of 12–24 fs^2 we calculate based on propagation of the cylindrical SPP modes for the wavelength range of our pulse.

While our measured decrease in SPP group velocity confirms the proposed general mechanism of adiabatic nanofocusing, our results suggest that its details sensitively depend on the exact geometry of the plasmonic taper. Together with more precise engineering of the tapered plasmonic device geometry, this should enable the realization of broadband SPP-based slow light applications.

We would like to acknowledge funding from the Department of Energy Division of Materials Sciences and Engineering (Grant No. DE-SC0002197), the National Science Foundation (NSF CAREER Grant No. CHE0748226), and a partner proposal by the Environmental Molecular Sciences Laboratory (EMSL), a national scientific user facility from the DOE's Office of Biological and Environmental Research at Pacific Northwest National Laboratory (PNNL). PNNL is operated by Battelle for the U.S. DOE under the contract DEAC06-76RL01830. We thank Samuel Berweger for valuable discussion and Ian Craig for help in tip fabrication.

References and Note

1. A. M. Steinberg, P. G. Kwiat, and R. Y. Chiao, Phys. Rev. Lett. **71**, 708 (1993).
2. D. Shafir, H. Soifer, B. D. Bruner, M. Dagan, Y. Mairesse, S. Patchkovskii, M. Y. Ivanov, O. Smirnova, and N. Dudovich, Nature **485**, 343 (2012).
3. L. Thévenaz, Nat. Photonics **2**, 474 (2008).
4. R. W. Boyd, J. Opt. Soc. Am. B **28**, A38 (2011).
5. Y. Huang, C. Min, and G. Veronis, Appl. Phys. Lett. **99**, 143117 (2011).
6. A. Karalis, J. Joannopoulos, and M. Soljačić, Phys. Rev. Lett. **103**, 043906 (2009).
7. A. Kocabas, S. S. Senlik, and A. Aydinli, Phys. Rev. Lett. **102**, 063901 (2009).
8. K. V. Nerkararyan, Phys. Lett. A **237**, 103 (1997).
9. A. Aubry, D. Y. Lei, A. I. Fernández-Domínguez, Y. Sonnefraud, S. A. Maier, and J. B. Pendry, Nano Lett. **10**, 2574 (2010).
10. A. J. Babadjanyan, N. L. Margaryan, and K. V. Nerkararyan, J. Appl. Phys. **87**, 3785 (2000).
11. M. Stockman, Phys. Rev. Lett. **93**, 1 (2004).
12. C. Ropers, C. C. Neacsu, T. Elsaesser, M. Albrecht, M. B. Raschke, and C. Lienau, Nano Lett. **7**, 2784 (2007).
13. C. C. Neacsu, S. Berweger, R. L. Olmon, L. V. Saraf, C. Ropers, and M. B. Raschke, Nano Lett. **10**, 592 (2010).
14. T. Söndergaard, S. M. Novikov, T. Holmgaard, R. L. Eriksen, J. Beermann, Z. Han, K. Pedersen, and S. I. Bozhevolnyi, Nat. Commun. **3**, 969 (2012).
15. C. Rewitz, T. Keitzl, P. Tuchscherer, J.-S. Huang, P. Geisler, G. Razinskas, B. Hecht, and T. Brixner, Nano Lett. **12**, 45 (2012).
16. B. Wild, L. Cao, Y. Sun, B. P. Khanal, E. R. Zubarev, S. K. Gray, N. F. Scherer, and M. Pelton, ACS Nano **6**, 472 (2012).
17. M. L. Balistreri, H. Gersen, J. P. Korterik, L. Kuipers, and N. F. van Hulst, Science **294**, 1080 (2001).
18. J. D. Mills, T. Chaipiboonwong, W. S. Brocklesby, M. D. B. Charlton, C. Netti, M. E. Zoorob, and J. J. Baumberg, Appl. Phys. Lett. **89**, 051101 (2006).
19. V. V. Temnov, U. Woggon, J. Dintinger, E. Devaux, and T. W. Ebbesen, Opt. Lett. **32**, 1235 (2007).
20. C. Neacsu, S. Berweger, and M. Raschke, Nanobiotechnology **3**, 172 (2007).
21. FIB milling performed with 30 kV, 3 nA Ga ion beam.
22. B. Xu, J. M. Gunn, J. M. D. Cruz, V. V. Lozovoy, and M. Dantus, J. Opt. Soc. Am. B **23**, 750 (2006).
23. R. Ruppin, Phys. Lett. A **340**, 299 (2005).
24. A. Wiener, A. I. Fernández-Domínguez, A. P. Horsfield, J. B. Pendry, and S. A. Maier, Nano Lett. **12**, 3308 (2012).
25. S. Berweger, J. M. Atkin, X. G. Xu, R. L. Olmon, and M. B. Raschke, Nano Lett. **11**, 4309 (2011).